Investigation of transfer correction for in-service inspection of coated steel welds using ultrasonic method

Chanitra Dumrongkit[1], Mai Noipitak[2*], Chanon Chiablam[2], Chonkarn Chiablam[2]

[1]Department of Production Engineering, Faculty of Engineering, King Mongkut's University of Technology Thonburi, Bangkok 10140, Thailand
[2]Materials and Nondestructive Testing Laboratory, King Mongkut's University of Technology Thonburi (Ratchaburi), Ratchaburi 70150, Thailand
***Corresponding author's email:** mai.noi@kmutt.ac.th
Received: 19 December 2022, Revised: 14 March 2023, Accepted: 6 May 2023

Abstract

Welding is commonly used for fabricating tanks or piping systems, and the weld joints are inspected immediately without painting. After all welds have passed the acceptance criteria, the welds are painted to prevent corrosion. Oil and gas pipelines, fuel tanks and associated steel structures are prone to stress and corrosion during operation. Additionally, unforeseen events such as accidents, earthquakes, or plate movements may result in damage, leading to leaks and cracks that can have significant environmental implications. Annual or periodic inspections are essential, as they require the removal of paint for evaluation because sound waves are attenuated by the paint layer. However, paint stripping is a costly and time-consuming process. This study aims to investigate the appropriate transfer correction for compensating the ultrasonic energy attenuation caused by coating thickness at different frequencies and probe angles for in-service inspection of coated steel weld joints using the ultrasonic method. Carbon steel A36 was used as the calibration specimen according to ASME 2021 criteria. Alkyd resin enamel paint was sprayed onto the specimens to simulate coating layers ranging from 0-900 microns in thickness. Weld joints were also used to simulate a lack of fusion discontinuity, with a design coating thickness of 0-400 microns. This study utilized frequencies of 2.25, 5 and 10 MHz, and the chosen angles included the normal angle (0 degrees) and angles of 45, 60 and 70 degrees. Increasing coating layer thickness resulted in greater energy attenuation and reflected energy when the coating layer was more than half of the sound wavelength. Attenuation was not observed in the normal probe at 2.25 MHz. However, at frequencies of 5 and 10 MHz, attenuation was observed starting from the designed coating thickness of 500 and 100 microns, respectively. Attenuation was present at all frequencies and angles for angle probes, increasing with angle and frequency. Equations and transfer corrections were provided to compensate for energy attenuation due to coating layers, thereby improving the accuracy of signal testing for weld joints in industrial applications. It may be possible to develop more reliable testing methods to ensure the safety and integrity of fuel transportation systems without the need for costly and time-consuming paint removal.

Keywords:
Coating Thickness; Energy Attenuation; Ultrasonic Testing

1. Introduction

Petroleum products have become an indispensable part of modern life, providing direct and indirect benefits such as energy, electricity generation, transportation services, and plastic and polymer applications, among others. The technology for delivering petroleum and energy products is of great

importance for improving the quality of life, developing the country, reducing inequality, and expanding the domestic economy. Currently, energy transportation for domestic and export purposes is carried out using various modes such as trucks, rails, tanker vessels, and pipelines [1, 2]. Safety and stability are critical factors in transportation, as unexpected events such as accidents, earthquakes, or tectonic plate movement may lead to cracks and leaks in pressure parts, which can cause explosions. Hydrocarbons [3], which are essential components of petroleum and natural gas, are organic compounds composed of hydrogen (H) and carbon (C). Burning hydrocarbon fuels releases carbon dioxide (CO2) into the atmosphere, contributing to the greenhouse effect or global warming. Manufacturing processes, chemical reactions of petroleum products, and leaks that result in atmospheric pollution release greenhouse gases, which have a significant impact on the environment and contribute to production costs. These emissions can be traded in the carbon market as carbon credits [4]. Thailand has ratified the Kyoto Protocol and established the Thailand Greenhouse Gas Management Organization to regulate and certify carbon-reduction projects and carbon credits. Even though emissions from leaks are small in comparison to manufacturing processes [5], reducing the risk of damage from leaks can still benefit society and the environment. Collaboration across sectors to reduce greenhouse gas emissions can contribute to sustainable development and promote a low-carbon society.

Tanks and pipes used for transporting petroleum products are fabricated using the welding process. However, welds are often the weakest points and may develop cracks during construction and service. These welds are immediately inspected by ultrasonic testing as they are not coated at the time. After acceptance, pipes and tanks are coated with epoxy and polyurethane materials to protect against rust and corrosion caused by the environment [6, 7], with a typical dry film thickness range of 85-300 microns for fuel tanks [8]. Ultrasonic testing is a widely used non-destructive testing method that assesses the internal integrity of materials by transmitting high-frequency sound waves through a medium or material and reflecting them back on a screen [9]. If the medium through which the sound wave travels is homogeneous, the reflected energy will not be attenuated and will be reflected from the back surface of the workpiece (back wall echo). A discontinuity trace that is equal in size to a wavelength or larger than a sound wave is reflected or absorbed by the discontinuity. These systems, including oil and natural gas pipelines, fuel tanks in the back of trucks and associated steel structures, are subject to stress and corrosion during use. As a result, annual or periodic inspections are necessary. In the evaluation of discontinuities within the weld joint using ultrasonic testing, the test is usually performed without coating or requiring the removal of coating [10]. The removal of coatings from structures can be expensive and time-consuming. If the test is performed through the coating using the original method, the results will be unreliable or the test may not be possible because ultrasonic waves travel through the coating thickness. A sound wave is attenuated by the reflections and refractions between the coating surface and the metal surface. Welds are inspected through the coating layer not only in the petroleum industry but also in other industries, such as structural work. Transfer correction is used in the surface preparation stage of API RP 2X recommendations for ultrasonic testing in offshore construction to adjust coatings that have a thin layer of thickness [11].

Predoi, M. V. and Petre, C. C. [12] investigated the attenuation of paint layers on thin-walled pipes by performing ultrasonic inspections through the paint layer. They used three wave types, longitudinal, torsional and flexional, on a 3 mm-thick steel pipe coated with 50-micron acrylic paint. The experiments showed that longitudinal wave attenuation increased with frequency, while the attenuation of torsional waves was nearly identical to that of longitudinal waves and increased more steadily with frequency. A high attenuation frequency domain was visible in the coated pipe. In another study, Crowley, B.M. [13]

investigated the effects of paint on phase-arranged ultrasonic testing (PAUT) and the attenuation of ultrasonic energy in bridge structural steel. Ultrasonic testing was carried out on the paint, the paint removed, and the paint removed and ground smooth surface using a 5 MHz frequency probe. The experimental results showed that test specimens with coated layers clearly affected ultrasonic testing. In compression waves, it was found that the coating layer amplifies the transmission signal and has more signal loss in the transverse wave. Ono, K. [14], has investigated the attenuation of sound waves in various engineering materials. The correlation between attenuation in various materials and the orientation of cold-rolled materials was investigated in this work. The attenuation coefficient was found to have changed due to the decreased dislocation density after annealing, resulting in lower attenuation for the annealed material. As frequency increases, the attenuation from the cold-rolled material in the transverse direction increases. Prior research reviews indicate that the effects of various frequencies and probe angles on ultrasonic inspection of weld joints through the coating layer without removing the paint have not been adequately addressed in the literature. This gap highlights the need for further investigation to develop more reliable testing methods that ensure the safety and integrity of fuel transportation systems such as pipes, tanks, or structures. Therefore, this study aims to bridge this gap by exploring the appropriate transfer correction to compensate for the ultrasonic energy attenuation caused by coating thickness at different frequencies and probe angles for in-service inspection of coated steel weld joints using the ultrasonic method. The testing was conducted without removing the coating, which improved the accuracy of the test results. These findings have important implications in determining whether a workpiece can be used continuously or requires repair or stopping to prevent potentially catastrophic consequences, such as leaks or explosions.

2. Experimental detail

2.1. Materials and methods

Carbon steel is widely used in all industries [15]. Therefore, there are frequent problems with using such materials. The specimen was a carbon steel plate ASTM standard grade A36 with dimensions 150 mm x 200 mm x 19 mm. Petroleum transportation mostly involves the use of carbon steel as a construction material, although grades other than A36 are available. Nevertheless, ASME correlates different material grades to P-numbers, and ASTM A36 is categorized under the same P number 1 as other grades used in the piping industry such as API- 5L (Refer to ASME Section V Article 4 and Section II Part D). The test specimen was prepared to create a calibration block for determining verification criteria, referencing the test specimen, or calibrating signals in accordance with ASME Section V Article 4 [16]. This code is used for non-destructive boiler and pressure vessel inspections, including ultrasonic testing. For a weld thickness not exceeding 25 mm, a calibration block with a thickness of 19 mm and a side drill hole of 2.5 mm must be prepared. Drilling 2.5 mm holes on each side at 1/4 and 1/2 of the thickness, as shown in Fig. 1. The coating thickness of structural steel is between 200 and 400 microns, while that of fuel tanks is between 85 and 300 microns [8]. The study utilized alkyd resin enamel paint as a coating material for the experimental specimens, which is a common type of industrial paint. If the paint used in the research is the same as that utilized in industry, the findings can be directly applied. The non-destructive evaluation of welds covered with a paint layer is performed using ultrasound in this study without the need for paint removal. Consequently, the experimental techniques previously described can be quickly adapted in the case of different coating materials being utilized. The paint is composed of a combination of alkyd resin, petroleum, xylene, dimethyl polysiloxane, and ethyl benzene. It was applied on the specimens using a spray technique with

varying layer thicknesses ranging from 0 to 900 microns. To control the paint thickness in this experiment, a method was employed in which the paint was sprayed once, and the thickness of the layer was measured using a micrometer. Subsequently, the paint was sprayed multiple times to determine the average thickness of the applied paint. This process was repeated to ensure that the paint thickness was approximately 70-100 microns with each spray. The amount of spraying required to achieve the desired paint layer thickness was calculated and the final paint thickness was verified by comparing the measurements of coated samples against their unpainted counterparts using a micrometer. The paint coating was designed for the paint thickness layer to cover the standard paint thickness used in actual work.

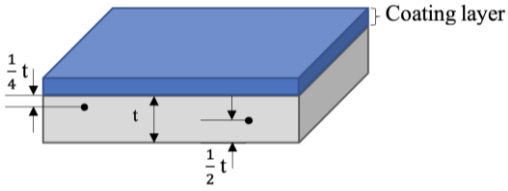

Fig. 1 Calibration block with coating thickness layer.

An ultrasonic testing device, the Olympus EPOCH 650, was used in this experiment (see Fig. 2). In industry, it is common practice to perform a test using a normal probe before testing with an angle probe. This is because the normal probe is used to check for discontinuities in base metal that are parallel to the surface of the specimen. Angle probes are used to check for discontinuities that are inclined to the surface or where a normal probe cannot be inspected [17, 18]. In the test, angle probes are used at 45, 60 and 70 degrees, which are the most common angles used in industrial testing. The probes for testing 2.25, 5 and 10 MHz frequencies, 0.5-inch focus transducer, were chosen because the frequencies affected the sensitivity of the test. The sensitivity [19] is the ability to find small defects, which can be calculated as follows:

$$\lambda = \frac{v}{f} \tag{1}$$

$$\text{Sensitivity} = \frac{\lambda}{2} \tag{2}$$

Where λ is the wavelength (mm), v is the sound velocity (mm/s), and f is the frequency (Hz).

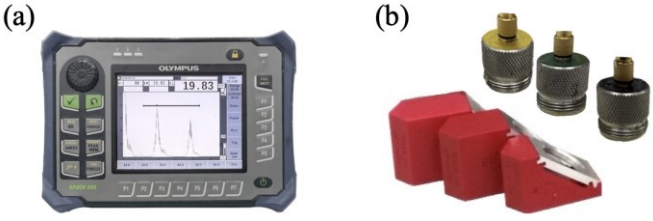

Fig. 2 (a) Ultrasonic testing device and (b) probes and wedges.

The ultrasonic test was carried out in pulse-echo mode and analyzed by using an A-scan image as a signal versus a time plot. The side drill hole of a known size was used as the default reference signal for the test, and its results were evaluated by peaking the indication signal of an uncoated specimen at 80% of the full-screen height (FSH). To compare the ultrasonic energy level compensation with the

increased layer thickness, the specimens with various coating layers were examined, and the indication signal peaked at a level of 80% FSH. The data for the normal probe was collected in the form of a back wall echo, while the angle probes were tested using a 2.5 mm side drill hole in the form of distance amplitude correction (DAC). As sound waves propagate through various materials, they undergo refraction at the boundaries between those materials. To determine the angles at the plastic wedge, the coating layer, and the steel specimen, Snell's law can be applied, as demonstrated in equation 3 and Table 1.

$$\frac{sin\theta_1}{sin\theta_2} = \frac{v_1}{v_2} \tag{3}$$

Where θ_1 is the angle of incidence (degree), θ_2 is the angle of refraction (degree), v_1 is the velocity of medium 1 (mm/s), and v_2 is the velocity of medium 2 (mm/s).

Table 1 The angle of incidence and angle of refraction on the coated specimen.

Angle probe	Incident angle at plastic wedge	Refracted angle at coating layer	Refracted angle at steel specimen
45	30.61	18.13	45.01
60	38.57	22.40	60.01
70	42.58	24.42	69.98

The direction of sound waves traveling into the specimen with the straight and angle beam probes is different, resulting in unequal distances traveled by the sound waves of the two probes. The sound path distance of the angle beam can be calculated from the Pythagorean formula, as shown in equations 4 and 5. The distance that the sound wave travels through the color layer is shown in Fig. 3 and Table 2.

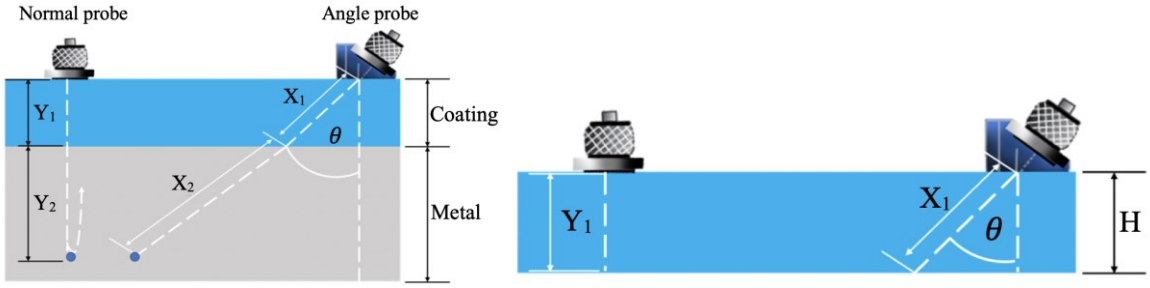

Fig. 3 Sound path in the coating layer of the normal and angle probes.

$$x_1 cos\theta = H \tag{4}$$

$$x_1 = \frac{H}{cos\theta} \tag{5}$$

Where x_1 is the sound path in the coating layer (mm), θ is the refraction angle in the coating layer (degree), and H is the coating thickness (mm).

Table 2 Sound path in coating thickness layers.

Coating thickness (microns)		Sound path in coating thickness layers (mm)							
		Normal probe		Angle probe 45°		Angle probe 60°		Angle probe 70°	
Design	Actual	Design	Actual	Design	Actual	Design	Actual	Design	Actual
0	0	-	-	-	-	-	-	-	-
100	92	0.100	0.092	0.105	0.097	0.108	0.100	0.110	0.101
200	193	0.200	0.193	0.210	0.203	0.216	0.209	0.220	0.212
300	307	0.300	0.307	0.316	0.323	0.324	0.332	0.329	0.337
400	387	0.400	0.387	0.421	0.407	0.433	0.419	0.439	0.425
500	513	0.500	0.513	0.526	0.540	0.541	0.555	0.549	0.563
600	583	0.600	0.583	0.631	0.613	0.649	0.631	0.659	0.640
700	737	0.700	0.737	0.737	0.776	0.757	0.797	0.769	0.809
800	787	0.800	0.787	0.842	0.828	0.865	0.851	0.879	0.864
900	957	0.900	0.957	0.947	1.007	0.973	1.035	0.988	1.051

The weld joints, 8.9 mm thick, were prepared with internal discontinuities to simulate defects for ultrasonic testing through the coating layer, as shown in Fig. 4. The experimental specimens were coated with the same alkyd resin enamel paint as the calibration block samples using a spray technique with different layers of 0, 100, 200, 300, and 400 microns, respectively. The actual coating thickness of the weld joints is presented in Table 3. The angle probes were used to inspect the weld joints for discontinuities through the coating layer.

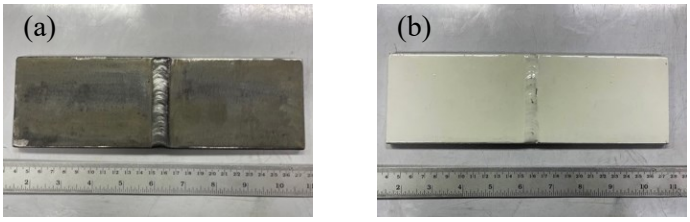

Fig. 4 Weld joint with simulated internal discontinuity. (a) weld joint without coating and (b) weld joint with coating thickness layer.

Table 3 Coating thickness of weld joints.

Coating thickness (microns)	
Design	Actual
0	-
100	85
200	168
300	223
400	378

The transfer correction value obtained from the calibration block specimen was used to inspect the weld joints in this research. The study establishes a criterion for assessing the discontinuity at 80% FSH. If the decibels are not compensated to remain within the designated energy level or within 80% FSH, the discontinuity may be considered acceptable. However, using energy compensation may result in the rejection of such discontinuities.

3. Results and Discussion

3.1. Normal probe

The specimen with a thickness of 19 mm underwent testing at frequencies of 2.25, 5 and 10 MHz. The signal transmitted and received in the specimen measured 38 mm. To find the transfer correction value for compensating the energy lost by high-frequency sound waves or decibels (dB) as they travel through the thickness layer of the coating, it was found that the near field distances at frequencies of 2.25, 5 and 10 MHz were 15.43, 33.39 and 68.19 mm, respectively. Signals at frequencies of 2.25 and 5 MHz were in the far field range, where the sound pressure was consistent. However, the signal at 10 MHz was in the near field range, where the sound pressure was not uniform [20].

Figure 5 shows the trend of ultrasonic energy compensation for the painted specimen with various coating layer thicknesses. It only demonstrates the effect of the signal with energy compensation due to the coated layer versus the uncoated target. This compensates the signal level to 80% FSH. The ultrasound energy level of the uncoated specimen is used as the energy compensation reference energy level. If any layer thickness has an energy level below the reference energy level, there is no need for energy compensation because there is sufficient energy to assess outcomes at 80% FSH. However, if any coating layer thickness has more energy than the reference level, it means that there is not enough energy to judge the effect at 80% FSH, judge the result at a lower energy level, or compensate energy up to 80% FSH. Due to the variations observed in the raw data measured through different coating layer thicknesses, a mathematical linear equation was used to build trend lines based on the energy compensation data. According to the test results, the frequency of the 2.25 MHz probe compensates for the energy of each layer less, with the start of energy compensation from energy attenuation due to the coating layer at a paint layer thickness of 957 microns. This is because the workpiece requires more energy than the uncoated specimen. The equation at 2.25 MHz could not be calculated in this experiment due to insufficient data. The energy compensation for each color layer was found to be greater at the 5 MHz frequency, with compensation starting at a paint layer thickness of 513 microns. It was found to be lower at the 10 MHz frequency, with compensation starting at a paint layer thickness of 92 microns. In this work, the sound wave velocity in the paint layer will be used to calculate the test sensitivity while considering the attenuation in the paint layer by referring to the sound velocity in paint materials with similar properties. The coating sound velocity for the longitudinal sound wave is 2730 m/s [21]. The sensitivities ($\lambda/2$) were calculated from the wavelengths (λ) of paint sound velocity at frequencies of 2.25, 5 and 10 MHz, which were 607, 273 and 137 microns, respectively.

When the sound wave travels through the coated workpiece, the difference in acoustic impedance (Z) of the paint and metal layers occurs [22]. Sound waves are partially transmitted and reflected, with the coating layer having less acoustic impedance than steel (Zpaint = 3.030 x 106 kg/m2s and Zsteel = 45.584 x106 kg/m2s). The differences in acoustic impedance of the two materials are quite different, resulting in less sound wave energy transmission and greater reflection [23]. The percentage of sound transmitted into the steel material is 23.38, and the reflectance percentage is 76.62. When the thickness

of the paint layer exceeds λ/2, more energy is required to be applied to the specimen. Due to the attenuation of sound wave energy, less energy is transmitted and more is reflected.

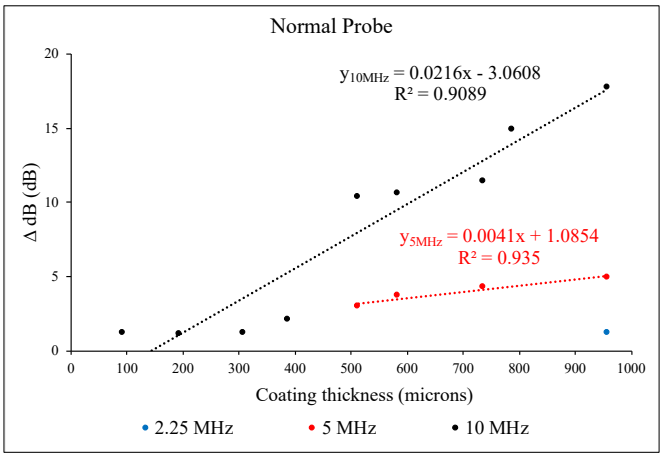

Fig. 5 The difference in decibels of a normal probe.

3.2. Angle probe

Figures 7-9 show the differences in decibels (dB) between the peak signal amplitude of a side drill hole of the specimen with various coating thicknesses and the default reference signal of an uncoated specimen. The tests were conducted using 2.25, 5 and 10 MHz frequencies of 45, 60 and 70 degrees angle probes, respectively. The same applies to the energy compensation data used to create the linear equations for the angle probe. The ultrasound energy level of the uncoated specimen is the energy compensation reference level. Ultrasonic energy compensation for a 45 degrees angle probe significantly increased when coating thicknesses ranging from 193 microns were considered at the 2.25 MHz frequency. The energy compensation significantly increased for a 45 degrees angle probe at 5 MHz frequency when coating thicknesses ranging from 92 microns were considered. A significant increase in energy compensation was observed for the 60 degrees angle probe at a coating thickness of 92 microns for the 2.25 MHz frequency. Energy compensation was found to significantly increase for coating thicknesses starting at 307 microns at a 2.25 MHz frequency of the 70 degrees angle probe. Additionally, the results of the test using the 5 MHz frequency probe showed a significant increase in energy compensation at coating thicknesses of 92 microns. On the other hand, the results of the test using the 10 MHz frequency probe showed a significant increase in energy compensation at coating thicknesses of 193 microns for all three angle probes: 45, 60 and 70 degrees. The near field distances in the wedge [24] at frequencies 2.25, 5 and 10 MHz were 38.77, 86.16 and 172.32 mm, respectively. The remaining near field distance in the steel specimen was calculated by subtracting the near field distance from the sound path in the wedge, as shown in Table 4. When the near field into the steel specimen was considered, all coating thicknesses and the sound path were found to be within the near field range. This is the range where the sound pressure is uneven, which may make the signal difficult to interpret because it may encounter signals that complement or cancel each other [20]. The near field effect on the specimen thickness has an impact, as shown in Table 4, when calculated according to the formula. When using a frequency of 2.25 MHz and a 45 degrees angle, if the specimen thickness is less than 14.14 mm, the inspection is carried out in the near field. Consequently, if the specimen thickness exceeds 14.14 mm, it will be examined in the far field. This range is appropriate for testing since the near field has no influence at that distance, leading to smoother

and more precise signal values. The typical distance for weld inspection is 1-2 legs [10], covering from the root to the cap of the weld, as depicted in Figure 6, which represents the path of the reflected sound wave from the weld. However, if the workpiece is thin, it may be possible to inspect the weld at a distance greater than two legs to compensate for the near field distance and ensure that the signal reflected from the weld is in the far field.

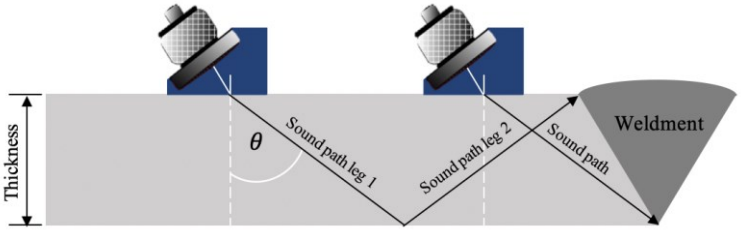

Fig. 6 Ultrasonic inspection of weld joint with 1 leg and 2 legs.

Table 4 Near field distance.

Frequency (MHz)	Near field (Wedge) (mm)	Angle (Degree)	Sound path (Wedge) (mm)	Near field (Steel) (mm)	Specimen thickness in near field distance (mm)
2.25	38.77	45	11	19.99	14.14
		60	18	14.95	7.48
		70	21	12.79	4.37
5	86.16	45	11	54.12	38.27
		60	18	49.08	24.54
		70	21	46.92	16.05
10	172.32	45	11	116.15	82.13
		60	18	111.11	55.56
		70	21	108.95	37.26

The coating sound velocity for a transverse sound wave is 1430 m/s [21], referring to the sound velocity in paint materials with similar properties. When the wavelengths at 2.25, 5 and 10 MHz frequencies were calculated, the sensitivities (λ/2) were found to be 318, 143 and 72 microns, respectively. The refraction angles in the paint layer were determined to be 18.13, 22.40 and 24.42 degrees, respectively, using Snell's law [20, 21] of the test probes at angles of 45, 60 and 70 degrees. The test results indicate that ultrasonic wave energy is attenuated as it passes through the medium, with transmission energy lost at the interface due to reflection, absorption, mode conversion and scattering [25]. Only a portion of the energy is transmitted through the interface between the paint layer and the steel layer, with the rest being reflected. As the inspection angle increases, resulting in the sound traveling through more layers of paint in the specimen, more attenuation from the coating layer occurs, which requires more energy to be supplied to the specimen, as shown in Table 1. Greater attenuation occurs when the paint layer thickness is greater than the sensitivity (λ/2), resulting in decreased energy transmission to the target and increased reflectivity. Different sound wave velocities in the material are a result of different mechanical properties. The transverse sound velocity is computed for the angle probe [21, 22]. It was found that the acoustic impedance of the paint was 1.587 x10^6 kg/m^2s and the acoustic impedance of the steel was 25.025 x 10^6 kg/m^2s. The acoustic impedance of the two materials

differ significantly, resulting in a percentage of sound transmitted into the steel material of 22.43 and a reflection percentage of 77.57. This reduces the transmission of sound wave energy and increases the reflection. The study found that sound waves passing through a paint layer and onto a steel layer with an angle of incidence greater than zero degrees from the normal line travel at angles of 45, 60 and 70 degrees. At the material interface, there will be a change in wave mode. The energy transmitted to the specimen is attenuated due to sound waves being reflected and refracted [23].

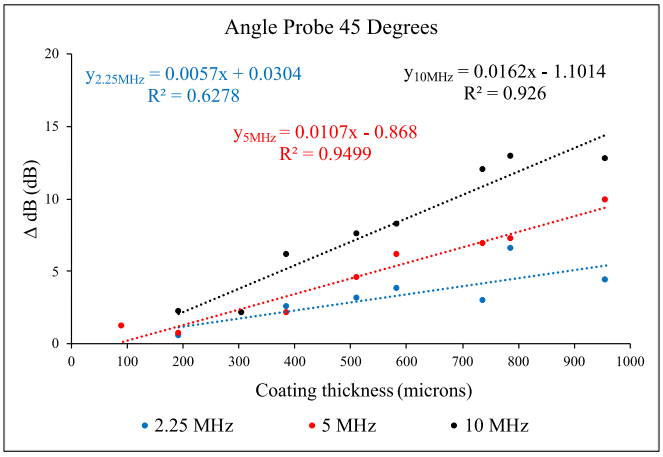

Fig. 7 The difference in decibels of an angle probe at 45 degrees.

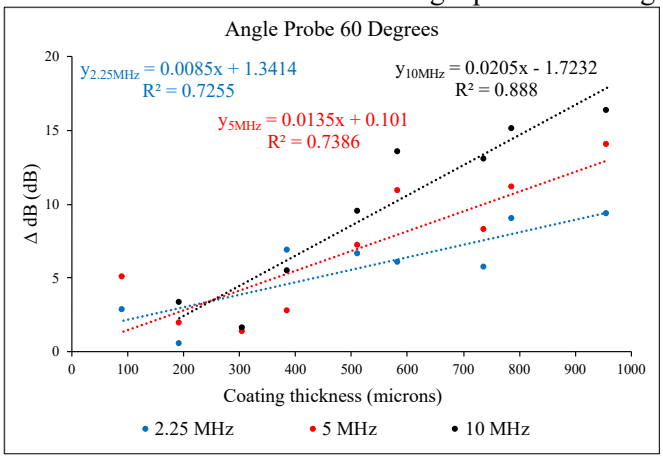

Fig. 8 The difference in decibels of an angle probe at 60 degrees.

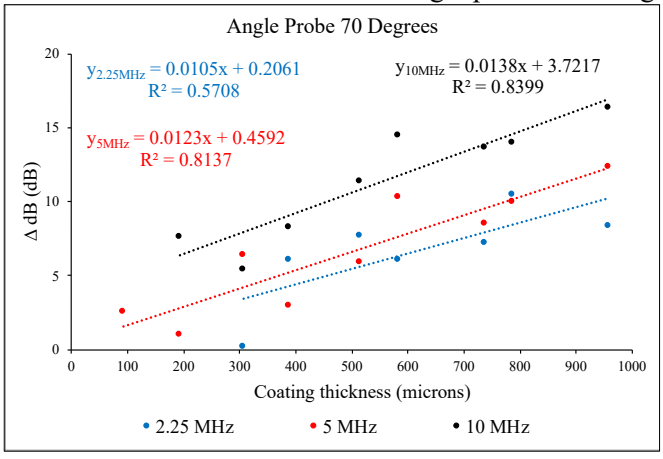

Fig. 9 The difference in decibels of an angle probe at 70 degrees.

3.3. Result of weld joint verification

Tests were performed on welded specimens that simulated internal discontinuities with coating thicknesses of 0-400 microns to verify the test results. Table 5 summarizes the linear equation for calculating ultrasonic energy compensation due to coating thickness attenuation. Using the linear equation to arrange the data to create a transfer correction for practical use in industry, as shown in Figures 10-13.

Table 5 Linear equations.

Test angle	Frequency (MHz)	Linear equation	R-square
Normal probe	2.25	-	-
	5	y = 0.0041x + 1.0854	0.935
	10	y = 0.0216x - 3.0608	0.909
Angle probe 45 degree	2.25	y = 0.0057x + 0.0304	0.628
	5	y = 0.0107x - 0.8680	0.950
	10	y = 0.0162x - 1.1014	0.926
Angle probe 60 degree	2.25	y = 0.0085x + 1.3414	0.726
	5	y = 0.0135x + 0.1010	0.739
	10	y = 0.0205x - 1.7232	0.888
Angle probe 70 degree	2.25	y = 0.0105x + 0.2061	0.571
	5	y = 0.0123x + 0.4592	0.814
	10	y = 0.0138x + 3.7217	0.840

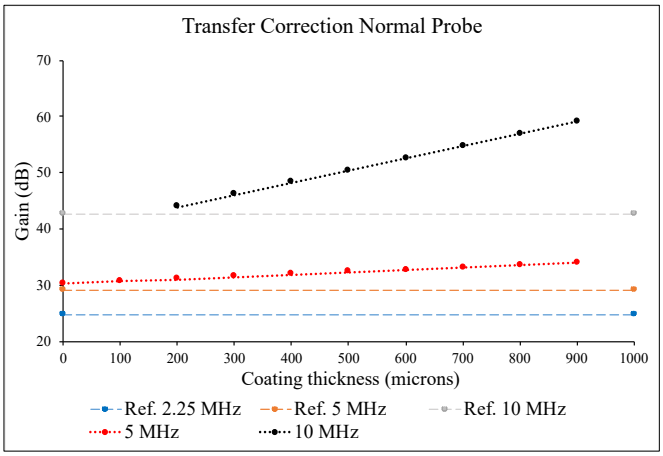

Fig. 10 Transfer correction of a normal probe.

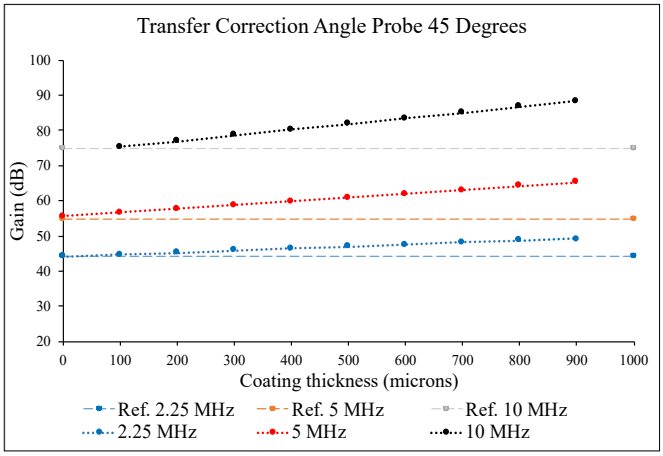

Fig. 11 Transfer correction of an angle probe at 45 degrees.

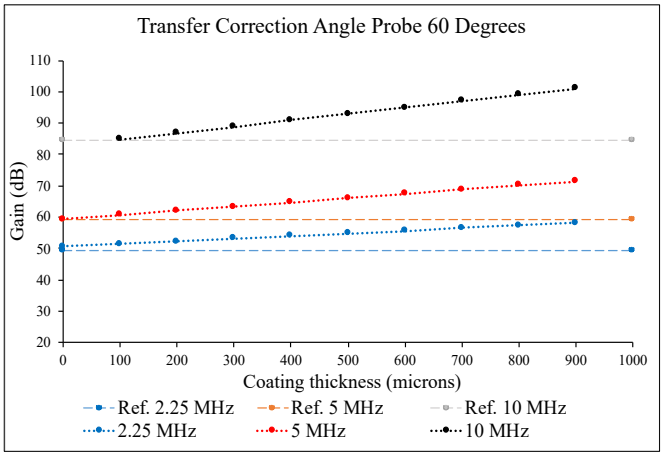

Fig. 12 Transfer correction of an angle probe at 60 degrees.

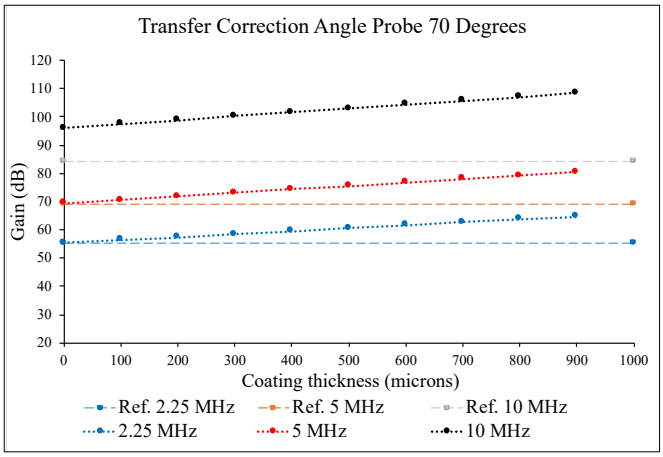

Fig. 13 Transfer correction of an angle probe at 70 degrees.

In this work, we are not concerned with attenuation from the microstructure but rather with attenuation from the coating layer. The microstructure of base metal is typically ferrite with small regions of pearlite at grain boundaries. After the welding process, the microstructure of the weld joint is composed of ferrite and pearlite, but with a smaller grain size in the heat-affected zone (HAZ) and a

larger grain size in the weldment. The ferrite-coarse pearlite microstructure absorbs more energy than the ferrite-fine pearlite microstructure. This effect is usually less pronounced in metal, where the absorption loss increases directly with the wave frequency [26]. The thickness of the paint was measured to be about 325 microns in the actual work. Therefore, to verify the transfer correction value for actual use, we simulated welding work with a maximum paint thickness of 0-400 microns. The process of calibrating the device for inspecting a weld joint with a coating thickness layer involves using a standard calibration block to set the initial energy signal at 80% FSH. After this step, the energy is adjusted using transfer correction values based on linear equations provided in Table 5 and Figures 10-13. Figure 14 represents an example of a practical application with a coating thickness of 100 microns. It was discovered that a discontinuity within the specimen could be found when testing with a non-coated weld joint, as shown in Fig. 14 (a). Additionally, during testing on a weld joint with a coated layer thickness of 100 microns, attenuation was observed when using the decibels obtained by testing with a calibration block without using transfer correction to compensate the energy (Fig. 14 (b)). According to the linear equation in Table 5 and the transfer correction in Fig. 11, for inspection using a frequency of 5 MHz and a probe angle of 60 degrees at a coating thickness of 100 microns, additional attenuation energy must be compensated up to 1.45 dB to achieve a level of energy sufficient to judge the result at 80% FSH. It was discovered that the aforementioned discontinuity could be seen when compensating for ultrasonic energy using the linear equation and transfer correction, as shown in Fig. 14 (c).

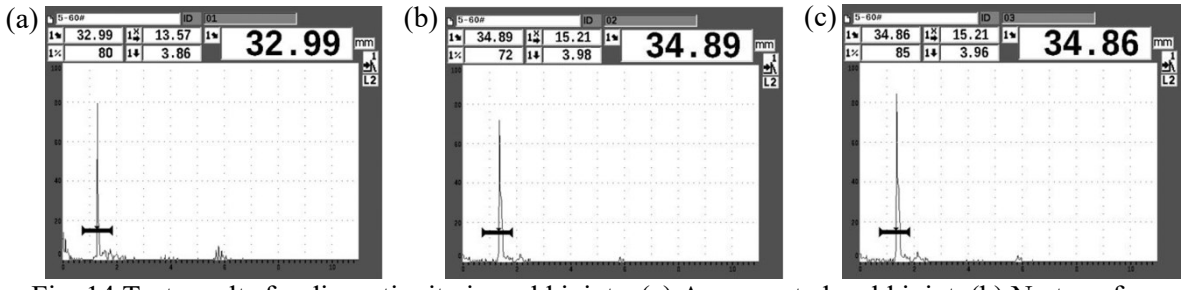

Fig. 14 Test results for discontinuity in weld joints. (a) An uncoated weld joint, (b) No transfer correction for inspection of the coated weld joint at 100 microns and (c) A signal after using transfer correction value.

4. Conclusion

Lower ultrasonic testing frequencies result in less attenuation due to longer wavelengths. However, the ability to detect small defects is reduced as it is proportional to half the wavelength. Conversely, high frequencies experience significant attenuation due to their shorter wavelengths, but they are capable of detecting small flaws effectively. Regarding the angle used in the test, different distances were traveled through the paint thickness layer depending on the angle. The greater the angle, the greater the distance and hence greater attenuation. However, large angles help in achieving the near field, which may cause the inspection to fall into the far field. Based on the study findings at a frequency of 2.25 MHz, a 70 degrees angle for inspection is not recommended due to the sound path's longer distance in the color layer at larger angles. The collected data also indicated a relatively low R-square value, which may lead to erroneous test results. Therefore, using a 60 degrees angle for inspection is suggested. The evaluation using the acceptance criteria may be inaccurate due to the attenuation caused by the paint thickness layer. The identified discontinuities or defects within the paint layer led to a low amplitude due to attenuation, which can result in the acceptance of the specimen evaluation with adverse effects on its future performance. The application of a linear equation and transfer correction in compensating

for ultrasonic energy enabled the examination of discontinuities under the weld and the thickness of the coating layer. Further research can build on these findings to optimize testing methods for weld joints and develop more precise and reliable non-destructive testing techniques.

Acknowledgements

The authors would like to acknowledge Ratchaburi Learning Park for probes and ultrasonic instruments and all of the MNDT members for their help and support.

References

[1] Library of congress. (n.d.). *Modes of Transportation. Oil and Gas Industry: A Research Guide*. Retrieved September 10, 2022, from https://guides.loc.gov/oil-and-gas-industry/midstream/modes

[2] Mohitpour, M. (2008). *Energy supply and pipeline transportation: challenges and opportunities: an overview of energy supply security and pipeline transportation*. New York, USA: ASME Press.

[3] MAN energy solutions. (2021). *Hydrocarbons*. Germany. Retrieved September 10, 2022, from https://www.man-es.com/discover/decarbonization-glossary---man-energy-solutions/hydrocarbons

[4] Kultida, B. (2019). The overview of carbon credit market in Thailand, *Sau journal of science & technology, 5*, 1-9. Retrieved September 13, 2022, https://ph01.tci-thaijo.org/index.php/saujournalst/article/view/184556

[5] TGO. (n.d.). *Monitoring and reporting guideline for Thailand voluntary emission trading scheme (Thailand v-ets): Refinery and petrochemical industry sector v.0.2. Thailand*. Retrieved September 13, 2022, from http://carbonmarket.tgo.or.th/admin/uploadfiles/ebook/content/a539e6a236/index.html

[6] PPT Public Company. (2015). *Natural gas pipeline installation*. Thailand.

[7] PPT Public Company. (2014). *Natural gas everyday*. Thailand. Retrieved September 10, 2022, from https://www.pttplc.com/th/Media/Publications/Knowledge/Naturalgasknowledge.aspx

[8] TOA-Chugoku paint. (n.d.). *Epoxy Tank Coating*. Retrieved May 24, 2022, from https://www.toa-chugoku.com

[9] Mahesh, L. K. S. (2009). *Ultrasonic Non Destructive Testing*. Retrieved July 15, 2022, from https://www.researchgate.net/publication/262809705

[10] American welding society. (2020). *Structural welding code - steel* (24th ed). USA: American Welding Society.

[11] API. (2004). *Recommended practice for ultrasonic and magnetic examination of offshore structural fabrication and guidelines for qualification of technicians.* Washington, D.C., USA: American Petroleum Institute.

[12] Predoi, M.V. & Petre, C.C. (2015). Thin Wall Pipe Ultrasonic Inspection Through Paint Coating, International Congress on Ultrasonics, 2015, *Physics Procedia, 70*(2015), 287-291.

[13] Crowley, B.M. (2018). *Ultrasonic Attenuation of Bridge Steels and Narrow-gap Improved Electroslag Welds*, Master of Science in Civil Engineering Thesis. Indiana, USA: Purdue University.

[14] Ono, K. (2020). A Comprehensive Report on Ultrasonic Attenuation of Engineering Materials, Including Metals, Ceramics, Polymers, Fiber-Reinforced Composites, Wood, and Rocks, *Applied Sciences, 10,* 7, pp. 2230.

[15] Sankara, P. (2014). *Corrosion Control in the Oil and Gas Industry*. London, UK: Gulf Professional Publishing.

[16] ASME boiler and pressure vessel committees (2021). *Boiler and pressure vessel code section V-nondestructive examination*. New York, USA: American Society of Mechanical Engineers.

[17] Berke, M. (2000). Nondestructive Material Testing with Ultrasonics - Introduction to the Basic Principles, *e-Journal of Nondestructive Testing (eJNDT), 5*(9). Retrieved July 23, 2022, from https://www.ndt.net/?id=540

[18] Olympus IMS (n.d.). *Ultrasonic Flaw Detection Tutorial*. Retrieved July 23, 2022, from https://www.olympus-ims.com/en/ndt-tutorials/flaw-detection/common-test-practices/

[19] Center of nondestructive evaluation (n.d.). *Waves*. Retrieved August 28, 2022, from https://www.nde-ed.org/Physics/Waves/WaveInterference.xhtml

[20] ASM International Handbook Committee. (1989). *ASM Handbook Volume 17: Nondestructive Evaluation and Quality Control*. Ohio, USA: ASM International.

[21] Peter, J. Sh. (2001). *Nondestructive Evaluation: Theory, Techniques, and Applications.* New York, USA: Marcel Dekker, Inc.

[22] Cheeke, J. D. N. (2002). *Fundamentals and Applications of Ultrasonic waves.* Florida, USA: CRC Press LLC.

[23] Steven, L. G. (2020). *Understanding Acoustics: An Experimentalist's View of Sound and Vibration (2nd ed)*, ASA Press.

[24] Ed, G., Robert, G., & Rick, M. (2016). Low velocity elastomer polymer wedges applied to TOFD, *e-Journal of Nondestructive Testing (eJNDT), 21*(5), 1-8. Retrieved October 5, 2022, from http://www.ndt.net/?id=19090

[25] Robinson, E. A., & Sven, T. (2008). *Digital imaging and deconvolution: the ABCs of seismic exploration and processing*, Tulsa, Oklahoma, USA: Society of Exploration Geophysicists.

[26] Boumerzoug, Z., Derfouf, C., & Baudin, T. (2010). Effect of welding on microstructure and mechanical properties of an industrial low carbon steel. *Engineering,* 2, 502-506. Retrieved September 15, 2022, from https://www.scirp.org/html/2246.html